Analyst

Accepted Manuscript

ROYAL SOCIETY OF CHEMISTRY

www.rsc.org/analyst

Analyst

RSCPublishing

ARTICLE

Two fluorescent Schiff base sensors for Zn^{2+}: the Zn^{2+}/Cu^{2+} ion interference

Cite this: DOI: 10.1039/x0xx00000x

Arturo Jiménez-Sánchez,[a] Benjamín Ortíz,[b] Vianney Ortiz Navarrete,[b] Norberto Farfán[c] and Rosa Santillan[a]*

Received 00th January 2012,
Accepted 00th January 2012

DOI: 10.1039/x0xx00000x

www.rsc.org/

Two simple and low cost 2,4-di-*tert*-butyl-6-[(1-hydroxycyclohexylmethylimino) methyl]phenol (**L1**) and 2-[{(1-hydroxylcyclohexyl)methylimino}methyl]phenol (**L2**) Schiff bases sensors exhibiting selectivity for Zn^{2+} in water : methanol (95 : 5, v/v, 10 mM HEPES) are described. **L1** and **L2** display an "off-on" fluorescent effect forming the **L1•Zn** and **L2•Zn** complexes, respectively. In the case of **L1•Zn**, the emission response is quenched by the addition of Cu^{2+} forming the respective **L1•Cu** complex; in spite of that, the fluorescence signal can be completely restored only by the addition of tartrate anions ($C_4H_4O_6^{2-}$) forming again **L1•Zn** *via* "off-on" *displacement approach*. However, in the case of **L2•Zn** no Cu^{2+} interference is observed, which is a typical problem for Zn^{2+} sensors. Here we describe that a very subtle structural change in the ligand when going from the *enol-imine* tautomer in **L1** to the *keto-enamine* tautomer in **L2** is enough to modulate the Zn^{2+}/Cu^{2+} selectivity. Also, the Zn^{2+} *vs* Cd^{2+} discrimination for **L1** and **L2** is proved. Moreover, we found that interaction between both **L•Zn** complexes and tartrate anion completely restored the free ligands by the ligand substitution mechanism even in a more efficient association than phosphate anions. Further, a second colorimetric response channel upon addition of Fe^{2+} was observed for **L1** and **L2**. Then, TD-DFT theoretical calculations were conducted in order to study the efficiency of the sensors to give different responses in the presence of such metal ions. Finally, **L2** sensor successfully detects Zn^{2+} in Jurkat cells cultured with and without Zn^{2+} enriched medium.

Introduction

The selective and sensitive detection of metal ions, anions, protons and guest molecules has become an area of intense research.[1-2] Recently, several chromophores / fluorophores have been designed for the detection of different metal ions.[3] However, one of the problems is that not a single optical sensor known to date is completely specific,[4] in particular for analytes in multi-component pollutants[5] where the use of several probes leads to complications such as metal ion interference, sample contamination and cross-talk.[6]

Particularly, the detection of metal ions of biological importance has attracted much attention. In this context, Zn^{2+} fluorescent sensors have acquired special interest. Zn^{2+} is an essential trace element and the second most abundant metal ion (after Fe^{2+}) in the human body,[7] and also one of the most common in natural environments.[8] Additionally, Zn^{2+} is involved in many pathological events such as Alzheimer and Parkinson's diseases, epilepsy and ischemic stroke;[9] it also plays an important role in cancer prevention.[10] However, the detection of Zn^{2+} requires high sensitivity and selectivity, particularly versus Cu^{2+}, the third most abundant metal ion in human body.[11] Unfortunately, the vast majority of Zn^{2+} sensors suffer from metal ion interference with Cu^{2+} ions[12] and in some cases Cd^{2+} also exerts interference,[13] making the sensor not really useful for continuous and large-time applications in real samples.

This problem is intensified by the fact that in cancer cells the concentration of Fe^{2+}, Zn^{2+} and Cu^{2+} changes tremendously, such that the concentration of Cu^{2+} can be the largest of these three ions. For example, the concentration of Fe^{2+}, Zn^{2+} and Cu^{2+} in the serum of the peripheral blood of healthy children and children with acute lymphocytic leukemia changes from 68, 103 and 114 μg/dL to 96, 136 and 328 μg/dL, respectively.[14] Therefore, a practical method for the determination of Zn^{2+} in biological samples must consider a large excess of Cu^{2+} and also the sensor must tolerate the presence of Fe^{2+}.

Regarding the Zn^{2+}/Cu^{2+} ion interference, Canary and coworkers described an approach to improve the selectivity of Zn^{2+} by controlling the stereochemistry and increasing the rigidity of the ligand scaffold of a series of piperidine tripod ligands.[15a] However, so far there have been very few reports of Zn^{2+} fluorescent sensors presenting an approach to improve the Zn^{2+} selectivity over Cu^{2+}.[15]

On the other hand, Schiff bases represent an interesting family of molecular sensors, since they exhibit excellent ligand properties and also involve easy and low cost synthetic methods.[16]

In this work we describe two fluorescent turn-on Schiff base sensors **L1** and **L2** (Figure 1) where the selectivity for Zn^{2+} ions

is analyzed against other metals including Cu^{2+} and Cd^{2+} in water : methanol (95 : 5, v/v, 10 mM HEPES). Here we report that **L1**, in spite of its Zn^{2+}/Cu^{2+} interference, is capable of detecting tartrate anions ($C_4H_4O_6^{2-}$) *via* Cu^{2+} *displacement approach*[17] after forming the **L1•Cu** complex. However, in the case of ligand **L2** having no *tert*-butyl groups in the aromatic ring, we demonstrate that this sensor is capable of detecting Zn^{2+} even in the presence of large amounts of Cu^{2+}. This subtle structural change is not involved in the ligand preorganization (as is commonly observed for *tert*-butyl substituted derivatives) but rather in their electronic properties, such that the *keto-enamine* structure is strongly favored, thus the imino-nitrogen lone pair is no longer available to coordinate with the highly azophilic Cu^{2+} ion. Further, sensors **L1** and **L2** showed no fluorescent response with Cd^{2+} and both of them can detect Fe^{2+} ions *via* a second-channel colorimetric response even in the presence of Fe^{3+}.

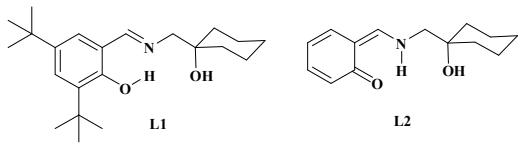

Figure 1. Structure of sensors **L1** and **L2**.

Experimental Section

General Information

All the solvents and reagents were spectroscopic and analytical grade. NMR spectra were recorded on a Jeol 500 MHz spectrometer and chemical shifts are recorded in ppm relative to $(CH_3)_4Si$ for ^1H and ^{13}C. Infrared spectra were obtained on an ATR-FTIR Varian Spectrometer. High resolution mass spectra were obtained with a TOF-Agilent G1969A spectrometer. Electronic absorption spectra were obtained using a Perkin Elmer LAMBDA 2S UV/VIS Spectrophotometer. The emission spectra and kinetic experiments were measured on a Varian Cary Eclipse fluorescence spectrometer. The compounds **L1** and **L2** were obtained from 1-aminomethyl-1-cyclohexanol hydrochloride and 3,5-di-*tert*-butyl-2-hydroxy-benzaldehyde (**L1**) and 2-hydroxy-benzaldehyde (**L2**) through a condensation reaction,[18] (see ESI†, Scheme S1).

Sample preparation and measurements

The Stock solution of **L1** was prepared by the following procedure: 3.4 mg (0.01 mM) of **L1** were dissolved in a water : methanol (95 : 5 v/v, 10 mL) solution to afford a 1 mM concentration, then 50 μL were taken and diluted with 4.95 mL of a 10 mM HEPES buffer solution to give a final concentration of 10 μM. Analogously, 2.3 mg (0.01 mM) of **L2** were dissolved in a water : methanol (95 : 5 v/v, 10 mL) solution, then, we followed the same procedure as **L1** to give a final concentration of 10 μM. Metal acetates $M(O_2CCH_3)_2$, where M = Zn^{2+}, Cd^{2+}, Co^{2+}, Cu^{2+}, Hg^{2+}, Ni^{2+}, Pb^{2+}, Ca^{2+}, K^+, Li^+, Fe^{2+} ($FeCl_2$ having 1mM HCl) and Fe^{3+} ($FeCl_3$), were dissolved in water. For anion experiments, Stock solutions were prepared in 10 mM HEPES buffer of different anions 10 μM, NaF, NaCl, NaBr, NaI, NaN_3, $NaHSO_3$, $NaNO_2$, Na_2S, $Na_2S_2O_3$, Na_2SO_3, Na_2CO_3, tartrate ($Na_2C_4H_4O_6^{2-}$), Na_2HPO_4, NaH_2PO_4 and Na_2ATP. A 10 mm quartz cuvette provided with a magnetic stirrer was used. After mixing the respective solution, UV-Vis and then fluorescence spectra were taken at 25ºC in a multicell holder electro-thermally controlled by peltiers. For the competition experiments with other metal ions the same solutions referred above were prepared, then $M(O_2CCH_3)_2$ were dissolved in water. Thus, for Zn^{2+} a solution having 3 mL of **L1** or **L2** (10 μM) and 12 μL of each metal ion (40 mM) to give 4 equivalents were stirred and mixed with 3 μL of a Zn^{2+} solution (10 μM, 1 equiv.). For Cu^{2+} a larger excess was used. Zn^{2+}/Cu^{2+} competition experiments were carried out with and without HEPES buffer solutions finding no significant differences in the UV-Vis and fluorescence responses. The *relative* quantum yields were obtained by using the experimental procedure reported in reference 19 using anthracene at 20 ºC as a reference ($\Phi_F = 0.27 \pm 0.03$, in ethanol).

Results and discussion

Zn^{2+} fluorescent response

The UV-Vis and fluorescence spectra were studied for **L1** and **L2** in the presence of Zn^{2+}, Cd^{2+}, Co^{2+}, Cu^{2+}, Fe^{2+}, Hg^{2+}, Ni^{2+}, Pb^{2+}, Ca^{2+}, K^+, Li^+ and Fe^{3+} where only Zn^{2+} resulted in the formation of a single florescence band. The observed fluorescence enhancement for receptor **L2** was *ca.* 3-fold superior to **L1**, exhibiting quite different optical properties, Figure 2.

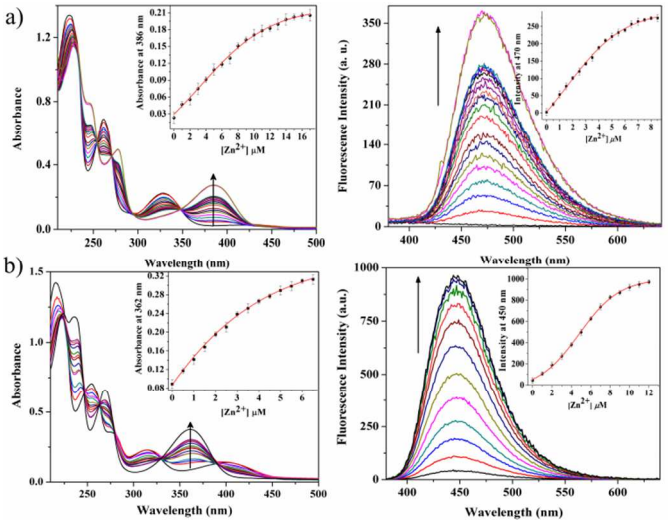

Figure 2. UV-Vis (left) and fluorescence (right) spectra upon 50 μM Zn^{2+} addition to: a) **L1** (10 μM, λ_{ex} = 327 nm) and b) **L2** (10 μM, λ_{ex} = 330 nm) in a water : methanol (95 : 5, v/v, 10 mM HEPES).

The fluorescence and UV-Vis spectra of **L1** and **L2** towards other metal ions are presented in Figure S1†. The absorption spectrum of **L1** shows one band at 330 nm, while **L2** exhibits two bands at 315 and 400 nm implying the presence of both *enol-imine* and *keto-enamine* structures. In addition, previously reported X-ray data also confirms the *keto-enamine* structure of **L2**.[18] Spectrophotometric titrations of most metal salts produced almost no change in absorption spectra; however, when Zn^{2+} was added to these solutions a new absorption band at 385 nm for **L1** and 360 nm for **L2** was observed. The fluorescence responses were also studied by increasing the concentration of the metal salts in the presence of **L1** and **L2**, Figure 2 and S1†. The emission spectrum of each pure receptor showed almost no fluorescence with a maximum difficult to find on excitation in the 220 to 400 nm range. As mentioned

before, among all examined metals, only the addition of Zn^{2+} produced an emission enhancement ($I - I_0 / I_0 = 35.2$ at λ_{ex} = 327 nm for **L1**; and 85.7 at λ_{ex} = 330 nm for **L2**), with a fluorescent quantum yield of $\Phi_F = 0.095$ for **L1·Zn** and Φ_F = 0.265 for **L2·Zn**, observing no change in emission wavelength with the subsequent additions.

The competition experiments did not show appreciable change with addition of other metal ions, Figure 3. Importantly, the selectivity of the sensors for Zn^{2+} in the presence of Cd^{2+} ions was completely superior, this is important due to the fact that Cd^{2+} is a transition metal with very similar chemical properties since $Zn^{2+}$and Cd^{2+} are both XII group elements having closed-shell d^{10} configuration, and as mentioned above Zn^{2+} is essential to many biological processes while Cd^{2+} is highly toxic in even low concentrations.[20] Thus, **L1** and **L2** discriminated Cd^{2+} from Zn^{2+}, which comprises a crucial characteristic for Zn^{2+} fluorescent sensors.[13]

Zn^{2+}/Cu^{2+} interference

In the case of **L1** the fluorescence spectra show that the presence of Zn^{2+} and Cu^{2+} in the same sample solution generated a metal ion interference such that no fluorescence signal is observed, this behavior could be attributed to the quenching ability of Cu^{2+} by means of an electron/energy transfer process given its paramagnetic properties and partially filled *d* subshell, Figure 3a. This result indicated a higher binding affinity for Cu^{2+} compared to Zn^{2+} ions (*see* below). However, anion-complex interaction experiments show that the formed **L1•Zn** complex can selectively recognize Cu^{2+} and S^{2-} ions. The Cu^{2+} ion quenches the fluorescence forming a new 'off-complex' **L1•Cu** which displaces Zn^{2+} ion, and the S^{2-} anion that recovers the fluorescence response by the return of Zn^{2+} to the receptor site forming again **L1•Zn**. This *"on-off-on"* response is not common for the metal-ion sensors reported in the literature and is of particular interest since no EDTA-type chelating agents were needed to recover the sensor, also giving the opportunity to use **L1•Zn** to detect S^{2-} anions. Thus, the reversibility and cyclability properties of **L1** as sensor were explored by testing a number of anions, corroborating that the signal response of **L1•Zn** can be restored from the **L1•Cu** "off-complex" upon addition of S^{2-} anions *via* Cu^{2+} *displacement approach*. In the *displacement approach* the **L1·Cu** "off complex" has no fluorescence due to the metal-ion induced fluorescence quenching mechanism; however, the S^{2-} anion displaces Cu^{2+} from the coordination sphere releasing **L1** into the solution and restoring the fluorescence by inducing the re-coordination with Zn^{2+}.

Furthermore, another anion recognition test was carried out for **L1•Zn** in order to completely recover the free ligand **L1**, finding that tartrate^{2-} anion is highly specific for binding Zn^{2+} in this system, Figure 3, see the *Reversibility processes* section for the detailed analysis. Thus, **L1** was able to detect both metals and selectively lose them by S^{2-} and tartrate addition, Figure 3a. However, although **L1** successfully operates in such a way that is possible to detect Zn^{2+}, Cu^{2+}, S^{2-} and tartrate^{2-} with almost no interference, care should be taken when a detailed quantitative analysis of Zn^{2+} is desired since *in-situ* Cu^{2+} concentration should preferably be known in order to avoid cross-talk and blank contamination problems.

On the other hand, for sensor **L2** no Cu^{2+} interaction was observed in the UV-Vis and fluorescence spectra when the competition experiment was carried out, Figure 3b and Figure S1b†, so that our proposal is that this Zn^{2+} selectivity can be

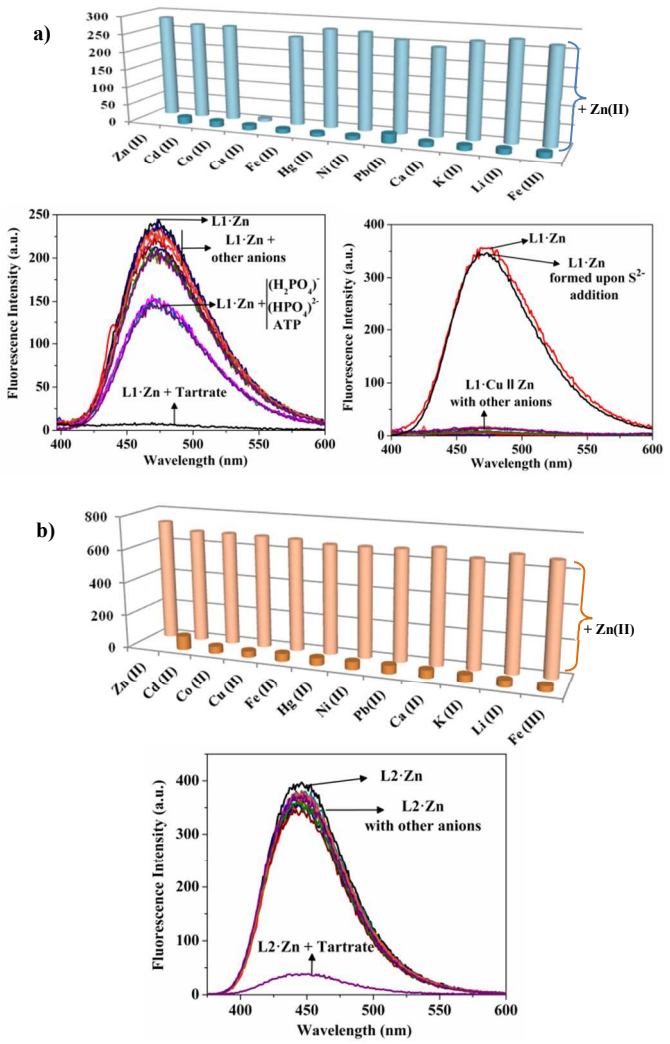

Figure 3. (a) Above: Fluorescence difference at 470 nm for **L1** (1 equiv.) in the presence of 4 equiv. of different metals (front bars) and competition with 2 equiv. of Zn^{2+} (back bars). Below: Competition with different anions to regenerate **L1** (left) and **L1•Zn** (right). (b) Above: Fluorescence difference at 445 nm for **L2** (1 equiv.) in the presence of 4 equiv of different metals (front bars) and competition with 1 equiv. of Zn^{2+} (back bars). Bellow: Competition with different anions to regenerate **L2**. Other anions: F^-, Cl^-, Br^-, I^-, N_3^-, HSO_3^-, NO_2^-, S^{2-} ,$S_2O_3^{2-}$, SO_3^{2-}, CO_3^{2-}, tartrate ($Na_2C_4H_4O_6^{2-}$), HPO_4^{2-}, $H_2PO_4^-$ and ATP.

attributed to the favored *keto-enamine* structure of the free ligand **L2** (Figure S2†) where the N_{imine} lone pair is no longer available to interact with copper since it is well known that the Cu^{2+} coordination is strongly dominated by its azophilic character in Nitrogen containing ligands.

Further, steady-state fluorescence kinetic measurements for both receptors were conducted in order to study the Zn^{2+}/Cu^{2+} interference and the sensor working time. The effect of reaction time on the fluorescence response in an **L1** or **L2** solution (3 mL, 10 μM) was first studied upon addition of a Zn^{2+} solution (6 μL, 20 mM) and then with the addition of a Cu^{2+} solution (12 μL of 40 mM for **L1** and 12 μL of 0.1 M for **L2**), with up to 80 points per second scans during 25 hours for **L1** and 90 hours for **L2** at a λ_{ex} = 327 nm, Figure S3†. For **L1** the fluorescence intensity profile showed a rapid enhancement when Zn^{2+} was added, then a slow fluorescence decrease was observed with

time, such that after 25 hours the fluorescence intensity decreased by 18%, then Cu^{2+} was added to the solution observing immediately the fluorescence quenching, Figure S3a†. In the case of **L2** the fluorescence intensity profile showed a rapid and strong enhancement upon Zn^{2+} addition and the formed **L2•Zn** complex did not exhibit any decreasing pattern during 5000 min (83.3 h) even when excess of Cu^{2+} was added to the solution, Figure S3b†.

Zn^{2+} and Cu^{2+} binding interactions

The binding stoichiometry was investigated by means of Job's plot. Changing the molar fraction from 0.0 to 1.0, the concentration of **L1**, **L2**, Zn^{2+} and Cu^{2+} in water : methanol (95 : 5, v/v, 10 mM HEPES) were maintained to 1 x 10^{-5} M. For **L1** the 1:1 complexes were observed. However, for **L2** the fluorescence intensity relation was not well fitted to a model involving the formation of a simple **L1•Zn** 1:1 complex. Then, for **L2** the best fit is shown as a blue line which has a minimum in the range 0.2–0.35 mole fraction and a break at 0.5 mole fraction, which can be attributed to the formation of the [Zn:**L2**] = 1:2 and 1:1 complexes, respectively (Figure 4). Moreover, the determined 1:2 complex concentration during titration were smaller (form 0 to 3.9 mM) and its absorbance was only significant at the 1:2 relation, Figure S4a†.

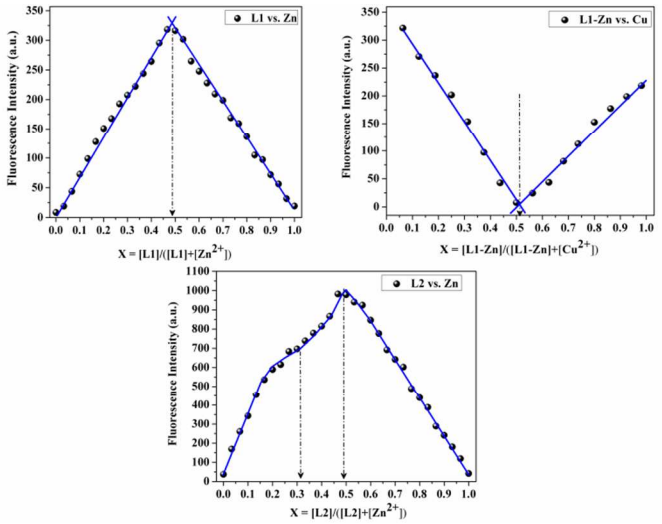

Figure 4. Job's plots obtained for the determination of the stoichiometry for **L1** vs. **Zn**, **L1**·**Zn** vs. **Cu** and **L2** vs. **Zn**. The final concentrations for each solution were 10μM in water : methanol, 90 : 5, v/v, 10 mM HEPES.

The detection limits based on the fluorescence response for **L1** and **L2** to Zn^{2+} were determined to be 7.25 x10^{-7} M and 3.08 x10^{-7} M on the basis of 3σ/K, respectively. The association constants for the 1:1 complexes (log K_a) on the basis of spectrometric titrations obtained with HyperQuad program[21] were estimated to be 5.277 ± 0.005 for **L1•Zn** and 8.54 ± 0.067 for **L1•Cu**. On the other hand, for **L2•Zn** we also found that the 1:2 complex exerts significant influence during titration (Figure S4a†). Then, we determined the log K_a values for both stoichiometries, 8.445 ± 0.078 and 10.813 ± 0.097 for 1:1 and 1:2 complexes, respectively. The weaker interaction between **L1** and Zn^{2+} leads to a higher dependence of the formed complex with the media. The same log K_a values were estimated by means of Hill plots, finding no significant variation (Figure S4†), 4.97 ± 0.57 for **L1•Zn** and 7.82 ± 0.33 for **L2•Zn** (1:1). In fact, solvent polarity and specific solvent interactions have an important effect, since in *iso*-propanol and DMSO no free ligand band is observed, while in non-polar solvents the coordination equilibrium tends toward free ligand formation until practically no complex formation in the non-polar protic chloroform, Figure S5†. Moreover, it is worth mentioning that the log K_a value for **L2•Cu** is extremely small, i.e. spectrophotometric titrations in methanol : water (50 : 50, v/v) with 40 mM NaCl, fit for a log K_a = 2.17 ± 0.52 at pH 7 and 3.10 ± 0.36 at pH 8. However, in (95:5, v/v, 10 mM HEPES) we observed almost no spectral changes, suggesting an extremely poor interaction, thus, the observed association constant value was log K_a = 1.74 with a very large error.

^{1}H NMR titration experiments were carried out in DMSO-d_6 to further understand the interaction between sensor **L1** with Zn^{2+}/Cu^{2+} ions, sensor **L2** with Zn^{2+} and both of them with Fe^{2+} since, as it was described, **L1** and **L2** were able to recognize Fe^{2+} *via* a second channel (colorimetric) response, in the case of Fe^{2+} we used a water solution (Figure S6†). For **L1** the hydroxylic proton in 4.29 ppm corresponding to the phenolic fragment vanished upon addition of 1 equivalent of Zn^{2+} while the hydroxylic proton in 14.33 ppm corresponding to the cyclohexyl fragment did not show any change. Moreover, a slight shift of the imine proton to lower frequency was observed. This result suggests that the coordination with Zn^{2+} is taking place with the phenolic oxygen atom and the imine nitrogen atom. Interestingly, titrations with Cu^{2+} or Fe^{2+} (separately) to **L1** produced the same binding interaction, supporting the idea that no Zn^{2+}/Cu^{2+} differentiation could be achieved by **L1**. On the other hand, we found that in sensor **L2** both hydroxylic protons (at 13.85 and 4.31 ppm, since in DMSO-d_6 the *enol-imine* structure is dominant) disappeared upon addition of 1 equivalent of Zn^{2+}. Again, a slight shift of the imine proton to lower frequency was observed, this suggests the coordination with the two oxygen atoms and the imine nitrogen atom, Figure S6†.

This result also indicates that even if the *enol-imine* structure is dominant in **L2**, the ligand structure is capable of promoting the interaction with both oxygen atoms. Further, the phenolic proton signal disappeared upon addition of Fe^{2+} to **L2**.

Influence of various anions on L1 and L2 recognition of metal cations.

As mentioned before, the reversibility in the recognition process of **L1** was studied by adding aqueous solution of different anions to a water : methanol (90 : 5, v/v, 10 μM HEPES) **L1•Cu** or **L1•Zn** solution. First, we studied the influence of NaF, NaCl, NaBr, NaI, NaN_3, $NaHSO_3$, $NaNO_2$, Na_2S, $Na_2S_2O_3$, Na_2SO_3, Na_2CO_3, tartrate ($Na_2C_4H_4O_6^{2-}$), Na_2HPO_4, NaH_2PO_4 and adenosine 5′-triphosphate disodium salt hydrate (Na_2ATP). Interestingly, the fluorescence properties of **L1•Cu** were only restored by adding S^{2-} anions (log K_a = 4.68 ± 0.03), where the "off-on" effect was evidenced as the emission intensity was increased with the S^{2-} addition until it was completely regenerated. This S^{2-} recognition with Cu^{2+} complexes has been well documented before.[3b,17a,22] In addition, other anions did not produce any appreciable spectral change, Figure 3a (right). At this point, the reversibility was highly efficient to regenerate the fluorescence properties by forming again the **L1•Zn** complex. Then, a new reversibility test was carried out for **L1•Zn** and **L2•Zn** in order to regenerate the free ligands **L1** and **L2**; here we proved the same set of

anions mentioned above observing an abrupt decrease in the fluorescence signal with tartrate^{2-} anion for **L1•Zn** (to give **L1**) but a slightly different fluorescence band in the case of **L2•Zn**. It is worth mentioning that while S^{2-} and tartrate substitute **L1** by the formation of CuS and tartrate-Zn species, however, the mechanism of tartrate interaction with **L2•Zn** resulted more complicated. As is observed in the course of spectrometric titrations, tartrate leads to a different fluorescence band, Figure 3b. In fact, limiting fluorescence at the saturation with tartrate is still higher than the **L2** free ligand fluorescence with an emission maximum 15 nm bathochromically shifted. Then, the **L2•Zn**-tartrate interaction is not only a result of ligand substitution, indeed, tartrate anion also may induce the formation of a **L2•Zn**-tartrate ternary complex. To confirm this observation spectrophotometric titrations were carried out (Figure S7†), unfortunately, we found practically no difference in the absorption spectrum of **L2** before and after addition of Zn^{2+} and tartrate. Only after adding tartrate^{2-} in a 3:1 molar ratio with respect to Zn^{2+}, the free ligand spectrum was recovered. This suggests that an **L2•Zn**-tartrate complex is formed and then after some tartrate excess the ligand substitution is achieved, eq 1.[23] See Figure S7†

(1)

The association constant for **L1•Zn**-tartrate to give **L1** was simply determined by wavelength-independent spectrometric data with a good non-linear fitting behavior due to the pure ligand substitution process, noticeably, a log K_a = 4.65 ± 0.08 value was obtained. However, in the case of **L2** sensor the Hyperquad program[21] was used in order to take into account partially soluble precipitate, emission-wavelength dependence in the titration curve and a more complex system where not only free ligand substitution by tartrate is taking place. Then, in the stability constant refinement performed for the 3 species *L2•Zn*, *L2•Zn-tartrate* and *Zn-tartrate* we determined a small contribution of the ternary specie to the titration curve, indeed, the log β values for *L2•Zn*, *L2•Zn-tartrate* and *Zn-tartrate* were 5.052 ± 0.30, 4.228 ± 0.31 and 12.727 ± 0.16, respectively. Additionally, since the high affinity between Zn^{2+} complexes towards phosphate anions is well established, we tested the phosphates HPO_4^{2-}, $H_2PO_4^-$ and ATP for the two receptors; however, we observed just partial fluorescence decrease having no change in absorption or emission wavelength, which indicates a weak interaction between phosphates and Zn^{2+} in these systems, Figure 3b (right) and S8†.

Colorimetric changes with Fe^{2+}

It is well known that Fe^{2+} ion is easily oxidized to Fe^{3+} ion in aerobic aqueous environments, such that, the optical sensing for specific ferrous ions is of great importance. However, there is a small amount of molecular sensors for these ions, and most of them are selective for Fe^{3+}, but few compounds can selectively detect Fe^{2+},[24] including Schiff base derivatives.[12c] In addition, colorimetric methods are also interesting because of the ease of monitoring the presence of the analyte, and although the sensitivity of this light absorption sensors is relatively low compared with the fluorescent detection, the alternation of both channels of detection could be very useful, especially when the light absorption leads to a low-energy electronic transition. Figure S9† shows the UV-Vis absorption spectra for sensors **L1** and **L2**, in both cases a new red-shifted broad band is generated upon Fe^{2+} addition, for **L1** the λ_{max} is observed around 580 nm while for **L2** is around 540 nm. However, it is worth mentioning that **L1** sensor does no exhibit any isosbestic point and the strong color change to gray could be a consequence of the red-shifted band added to the isotonic increase in the general absorption spectrum (an average of several colors). On the other hand, **L2** turns to a violet color upon interaction with Fe^{2+} where several isosbestic points are observed (438, 384, 258, 243 and 230 nm). Importantly, the isotonic band pattern allows a well-defined red-shifted band in 540 nm which causes a defined color change to violet.

Then, during the competition experiments we also observed a color change in the case of Fe^{2+} ions for **L1** changing from colorless to gray. However, in the case of **L2** a *ca.* four excess of Fe^{2+} equivalents were needed to change to a violet color, Figure S9b,c†.

pH profiles of L1 and L2

The pH profiles from spectrophotometric titrations are shown in Figure S10†. In the acid region **L1** exhibits two isosbestic points at 315 and 340 nm accompanied by slight changes in the absorption band pattern which resulted adequate to determine the corresponding pK_a value of 3.19±0.03. Interestingly, this pK_a value is relatively more acidic than that reported for most of the Schiff bases,[25] typically having a pK_a ~ 4. In the case of **L2** two isosbestic points at 325 and 380 nm were observed, where the absorption band around 400 nm corresponding to the *keto* form completely disappears because of the protonation of the *keto* group to give the *enol* form. Then, a pK_a value of 4.09±0.02 was obtained. This results suggest that **L2** exists predominantly in the *keto-enamine* form around neutral pH, and protonation of the *keto* oxygen (with *enamine* deprotonation) must necessarily occur before metal-coordination. Consequently, the nitrogen lone pair of **L2** will never be available to interact with Cu^{2+} ion in a wide range of pH.

On the other hand, in the basic region **L1** shows *keto* formation due to de-protonation of the phenolic oxygen as can be seen from the formation of the absorption band around 400 nm. Importantly, for **L1** a two-pK_a spectral profile was found, indicating the presence of the two hydroxylic deprotonations. Thus, we calculated a first pK_a value of 10.62 ± 0.12 due to the $OH_{phenolic}$ deprotonation and a second pK_a value of 12.91 ± 0.05 due to the $OH_{cyclohexanol}$ deprotonation. Figure S10a† (right) shows the band around 410 nm which corresponds to the weak formation of the *keto* form for **L1**. In the case of **L2** a one-pK_a spectral profile was found, with a pK_a value of 13.21±0.07 corresponding to the $OH_{cyclohexanol}$ deprotonation. However, in this case a blue-shifting in the band around 400 nm was observed at pH close to 12. Also, it is worth mentioning that only **L2** sensor exhibited fluorescence in the basic region further confirming that coordination with Zn^{2+} occurs with $OH_{cyclohexanol}$ deprotonation. On the other hand, selectivity towards Zn^{2+} ions is strongly affected by the fact that the N_{imino} of **L1** is fully available to coordinate with Cu^{2+} ion and the *enol-imine* form is present in a wide range of pH.

Intracellular Zn^{2+} detection of L2

We further studied whether the sensor **L2** detects Zn^{2+} in a cell line. Thus we examined the fluorescence response in Jurkat

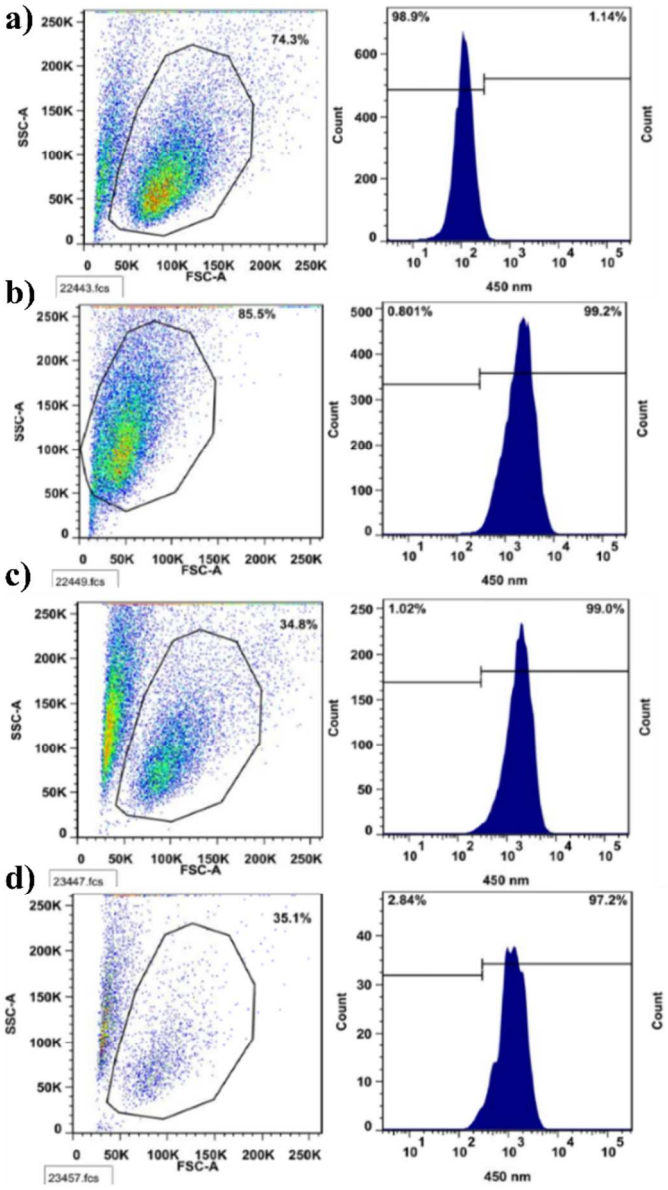

Figure 5. **L1** sensor detecting intracellular Zn^{2+} ions. Jurkat cells were cultured in the presence of 20 μM of a) Zn^{2+}, b) Zn^{2+} + **L2** after 30 min of incubation, c) Zn^{2+} + **L2** after 24 h incubation and d) **L2** for 30 min. Dot plots show forward scatter (FSC-A) *vs*. side scatter (SSC-A) and histograms show fluorescence intensity at 450 nm. Gated cells were selected according to side (FSC-A) and complexity (SSC-A) and emission of fluorescence at 450 nm was analyzed on live cells (histograms). Dead cells were excluded during acquisition by using propidium iodide (PI).

cells incubated with Zn^{2+} before and after incubation with an equimolar amount of **L2** sensor. The Jurkat cells were cultured in RPMI 1640 medium supplemented with 7% of fetal bovine serum (FBS) and 20 μM of $Zn(OAc)_2$. After 4h incubation period, the excess of Zn^{2+} was removed by centrifugation and afterward cells were incubated during 30 min with 20μM of **L2**. Then, cells were analyzed in a FACS (fluorescence-activated cell sorting).[26] Before the FACS analysis, 1% of propidium iodide (PI) was added to exclude dead cells. PI is a molecule that permeates dead cells and it fluoresces at 650-730 nm after excitation with a UV laser. For this reason it was possible to determine the fluorescence of the sensor **L2** at 450 ± 50 nm only in viable Jurkat cells. The FACS analysis data indicates a mean fluorescence intensity of 10^2 a. u. for the cells incubated only with Zn^{2+} ions (Figure 5a) but a strong fluorescence in Jurkat cells incubated with both, Zn^{2+} and **L2** sensor (10^3 a. u.), either after 30 min or 24 hrs of incubation (Figure 5a and 5c). A similar result was obtained from cells incubated only with the free **L2** sensor (Figure 5d) or Cu^{2+} (Figure S12†). These data demonstrate that intracellular Zn^{2+} ions induce a fluorescence response of **L2** and remarkably endogenous Zn^{2+} ions are able to trigger the response of **L2**. The aforementioned highlights the high selectivity and sensitivity of **L2** towards Zn^{2+} in living cells.

Theoretical calculations

Theoretical calculations were conducted to get insight into the sensing properties of receptors **L1** and **L2** by DFT with Polarizable Continuum Model[27] (for water) as performed in the Gaussian 09 code,[28] at a PBE0/6-31G(d) level of theory. Thus, TD-DFT/IEF-PCM were performed in order to understand the intramolecular charge transfer (ICT) properties present in the receptors, since ICT properties of the receptor are one of the main design elements to achieve sensitivity with the desirable charge distribution properties. The analysis on the electron density characteristics upon excitation of the receptors **L1** or **L2** as defined in refs 29 and 30 is presented in Figure S13†. Although TD-DFT provides a good benchmark in the determination of spectroscopic properties due to the accurate description of ground and excited potential energy surfaces, in most of the cases, conventional TD-DFT results in a description of an excited state in terms of several single electronic excitations from an occupied to a virtual orbital. Fortunately, the various contributions to the electronic excitation can be clarified by a Natural Transition Orbital (NTO) analysis,[31] which provides a compact orbital representation of the electronic transition through a single configuration of a *hole* and *electron* interaction. Consequently, the photoinduced electron transfer process is not depicted by a simple change in the elementary molecular orbital occupancy, but in a hole – electron distribution. Then, to have a better understanding on the sensor mechanism, we proposed sensor **L2** as a model compound representing an interaction scheme with both, Zn^{2+} and Cu^{2+}. NTO distributions for **L1** are presented in Table S1†. Figure 6 shows the NTO single electronic transitions for **L2**, **L2•Zn** and **L2•Cu**, providing the NTO coefficients (*w*) which represent the extent to which the electronic excitation can be written as a single excitation. Thus, for compound **L1** the hole and electron corresponding to the HOMO-LUMO level are localized along the salicylidene imine moiety with a $\pi \rightarrow \pi^*$ (*Sal*-$\pi \rightarrow$ *Sal*-π^*) character, a similar behavior was found for other NTO pairs corroborating a displacement of charge as confirmed by the calculated CT parameters. Therefore, in the Zn^{2+} complex the electron is transferred from the Zn ($d_{x^2-y^2}$)-π *hole* orbital to the salycilidene imine moiety (*Sal*-π^*) *electron* orbital resulting in a singlet metal to ligand charge transfer process (^{1}MLCT) which disfavors the ICT process of the free ligand and promotes fluorescence. However, in the case of the Cu^{2+} complex the electron transfer from the Cu^{2+} center to the photoexcited sensor (**L2***) is feasible, inducing the nonradiative deactivation of **L2***.[32] Other low-lying electronic transitions correspond to hole – electron interactions involving all the ligand structure (*all*-$\pi \rightarrow$ *all*-π^*).

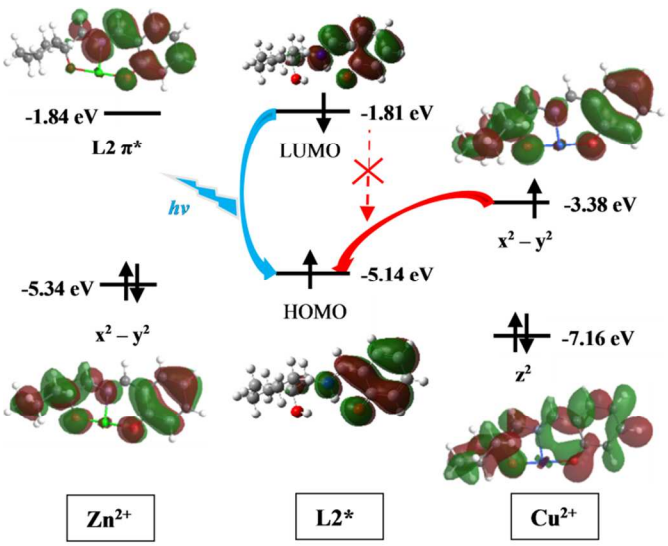

Figure 6. Schematic representation of the fluorescent sensing mechanism showing the Molecular Orbital contribution; Oscillator strength (f); transition wavelength (nm) and energy (eV) values and NTO coefficient (*w*) for the free ligand **L2**, **L2•Zn** and **L2•Cu** according to Table S1†.

Conclusions

We have explored the properties of two Schiff bases capable of sensing submicromolar quantities of Zn^{2+}. Although compound **L1** behaves similarly to most of previously reported Zn^{2+} sensors when Cu^{2+} ions are present, compound **L2** allows the fluorometric detection of Zn^{2+} having no Cu^{2+} interference. These results demonstrate that a subtle change in the ligand structure promoted the displacement in the tautomeric equilibrium from *enol-imine* to *keto-enamine*, altering the binding mode towards Zn^{2+} and Cu^{2+} metal ions, such that an interesting Zinc-Copper discrimination was achieved by the sensor **L2**. Fluorescence competition experiments show that **L1** displays a Zn^{2+}/Cu^{2+} ion interference by forming **L1•Cu**; however, this problem could be solved due to its high selectivity to recognize S^{2-} anions *via* Cu^{2+} *displacement approach* to regenerate **L1•Zn**. Moreover, the sensors can be completely regenerated from **L•Zn** complexes by tartrate anion addition but not by inorganic or organic phosphates which typically associate Zn-complexes. In addition, **L1** and **L2** presented a second colorimetric response channel to detect Fe^{2+} ions having no response to Fe^{3+}. Further, **L2** was able to map endogenous (natural) Zn^{2+} even in the presence of exogenous Cu^{2+} in Jurkat human cells.

Acknowledgements

The authors acknowledge the financial support of CONACyT and PAPIIT 214513 and also supercomputing Xiuhcoatl cluster administration of Cinvestav for the computational resources.

Notes and references

[a] Departamento de Química and [b] Departamento de Biomedicina Molecular, Centro de Investigación y de Estudios Avanzados del IPN, CINVESTAV, Apdo., Postal 14-740, México, D. F., 07000, México. E-mail: rsantill@cinvestav.mx;
Fax: +52 555-747-3389; Tel: +52 555-747-3725

[c] Facultad de Química, Departamento de Química Orgánica, Universidad Nacional Autónoma de México, México, D.F., 04510, México

† Electronic Supplementary Information (ESI) available: [UV-vis, Fluorescence, HRMS, ^{1}H and ^{13}C NMR spectra, can be found via the Supplementary Content section of the article webpage]. See DOI: 10.1039/b000000x/

1 (a) I. Leray and B. Valeur, *Eur. J. Inorg. Chem.,* 2009, 3525; (b) A. P. de Silva, *J. Phys. Chem. Lett.*, 2011, **2**, 2865; (c) A. P. de Silva, H. Q. N. Gunaratne, T. Gunnlaugsson, A. J. M. Huxley, C. P. McCoy, J. T. Rademacher and T. E. Rice, *Chem. Rev.*, 1997, **97**, 1515; (d) B. Valeur, *Molecular Fluorescence. Principles and Applications,* Wiley-VCH, 2002.

2 (a) H. F. Higginbotham, R. P. Cox, S. Sandanayake, B. A. Graystone, S. J. Langford and T. D. M. Bell, *Chem. Commun.,* 2013, **49**, 5061; (b) M. I. J. Stich, L. H. Fischer and O. S. Wolfbeis, *Chem. Soc. Rev.,* 2010, **39**, 3102; (c) S. M. Borisov and O. S. Wolfbeis, *Chem. Rev.,* 2008, **108**, 423; (d) A. Ito, S. Ishizaka and N. Kitamura, *Phys. Chem. Chem. Phys.,* 2010, **12**, 6641; (e) V. Luxami and S. Kumar, *RSC adv.,* 2012, **2**, 8734; (f) X. F. Yang, Y. X. Guo and R. M. Strongin, *Angew. Chem. Int. Ed.,* 2011, **47**, 10690; (g) Z. X. Li, L. F. Zhang, L. N. Wang, Y. Guo, L. H. Cai, M. M. Yu and L. H. Wei, *Chem. Commun.,* 2011, **47**, 5798; (h) Z. Guo, W. Zhu, L. Shen and H. Tian, *Angew. Chem. Int. Ed.,* 2007, **46**, 5549; (i) D. Maity and T. Govindaraju, *Chem. Commun.,* 2012, **48**, 1039; (j) S. Nagl and O. S. Wolfbeis, *Analyst,* 2007, **132**, 507.

3 (a) M. Alfonso, A. Tárraga and P. Molina, *Inorg. Chem.*, 2013, **52**, 7487; (b) Y. Chen, C. Zhu, J. Cen, J. Li, W. He, Y. Jiao and Z. Guo, *Chem. Commun*., 2013, **49**, 7632; (c) X. Chen, X. Meng, S. Wang, Y. Cai, Y. Wu, Y. Feng, M. Zhu and Q. Guo, *Dalton Trans.*, 2013, **42**, 14825; (d) W. H. Ding, W. Cao, X. J. Zheng, D. C. Fang, W. T. Wong and L. P. Jin, *Inorg. Chem.*, 2013, **52**, 7320.

4 O. S. Wolfbeis, *Angew. Chem. Int. Ed.*, 2013, **52**, 9864.

5 (a) H. Lu, Z. Xue, J. Mack, Z. Shen, X. Z. You and N. Kobayashi, *Chem. Commun.*, 2010, **46**, 3565; (b) M. Shellaiah, Y. H. Wu, A. Singh, M. V. Ramakrishnam Raju and H. C. Lin, *J. Mater. Chem. A*, 2013, **1**, 1310; (c) X. Wan, S. Yao, H. Liu and Y. Yao, *J. Mater. Chem. A*, 2013, **1**, 10505.

6 J. J. Lavigne and E. V. Anslyn, *Angew. Chem. Int. Ed.*, 2001, **40**, 3118.

7 (a) C. J. Frederickson, J. Y. Koh and A. I. Bush, *Nat. Rev. Neurosci.,* 2005, **6**, 449; (b) M. Stefanidou, C. Maravelias, A. Dona and C. Spiliopoulou, *Arch. Toxicol.,* 2006, **80**, 1; (c) D. S. Auld, *Adv. Chem.,* 1979, **172**, 112.

8 (a) H. Kozlowski, A. Janicka-Klos, J. Brasun, E. Gaggelli, D. Valensin and G. Valensin, *Coord. Chem. Rev.,* 2009, **253**, 2665; (b) M. Stefanidou, C. Maravelias, A. Dona and C. Spiliopoulou, *Arch. Toxicol.,* 2006, **80**, 1.

9 (a) A. I. Bush, W. H. Pettingell, G. Multhaup,; M. Paradis, J. P. Vonsattel,. J. F. Gusella, K. Beyreuther, C. L. Maeters and R. E. Tanzi, *Science* 1994, **265**, 1464; (b) V. Bhalla, Roopa, M. Kumar, *Dalton Trans.,* 2013, **42**, 975.

10 (a) A. S. Prasad, F. W. J. Beck, D. C. Snell and O. Kucuk, *Nutr. Cancer,* 2009, **61**, 879; (b) A. S. Prasad and O. Kucuk, *J. Am. Coll. Nutr.*, 1998, **17**, 542.

11 (a) R. Uauy, M. Olivares and M. Gonzalez, *Am. J. Clin. Nutr.* 1998, **67**, 952; (b) L. Banci, I. Bertini, K. S. McGreevy and A. Rosato, *Nat. Prod. Rep.,* 2010, **27**, 695; (c) E. Gaggelli, H. Kozlowski, D. Valensin and G. Valensin, *Chem. Rev.,* 2006, **106**, 1995.

12 For a very interesting sensors related to Zn^{2+}/Cu^{2+} interference: (a) C. Zhang, Z. Liu, Y. Li, W. He, X. Gao and Z. Guo, *Chem. Commun.*, 2013, **49,** 11430; (b) H. G. Lee, K. B. Kim, G. J. Park, Y. J. Na, H. Y. Jo, S. A. Lee and C. Kim, *Inorg. Chem. Commun.*, 2014, **39**, 61; (c) K. B. Kim, H. Kim, E. J. Song, S. Kim, I. Noh and C. Kim, *Dalton Trans.*, 2013, **42**, 16569; (d) L. Tang, J. Zhao, M. Cai, P. Zhou, K. Zhong, S. Hou and Y. Bian, *Tetrahedron Lett.*, 2013, **54**, 6105; (e) S. Zhu, J. Zhang, J. Janjanam, G. Vegesna, F. T. Luo, A. Tiwari and H. Liu, *J. Mater. Chem. B*, 2013, **1**, 1722; (f) N. Narayanaswamy, D. Maity and T. Govindaraju, *Supramol. Chem.*, 2011, **23**, 703; (g) B. K. Paul, S. Kar and N. Guchhait, *J. Photochem. Photobiol. A*, 2011, **220**, 153; (h) Y. Liu, Q. Fei, H. Shan, M. Cui, Q. Liu, G. Feng and Y. Huan, *Analyst*, 2014, **139**, 1868; (i) Z. Li, L. Zhang, L. Wang, Y. Guo, L. Cai, M. Yu and L. Wei, *Chem. Commun.,* 2011, **47**, 5798; (j) S. C. Burdette and S. J. Lippard, *Inorg. Chem.*, 2002, **41**, 6816; (k) J. Jiang, H. Jiang, X. Tang, L. Yang, W. Dou, W. Liu, R. Fang and W. Liu, *Dalton Trans*., 2011, **40**, 6367; (l) Y. Ikawa, M. Takeda, M. Suzuki, A. Osuka and H. Furuta, *Chem. Commun.*, 2010, **46**, 5689. (m) H. Xiao, K. Chen, N. Jiang, D. Cui, G. Yin, J. Wang and R. Wang, *Analyst*, 2014, **139**, 1980; n) D. H. Kim, Y. S. Im, H. Kim and C. Kim, *Inorg. Chem. Commun.*, 2014, **45**, 15.

13 For Zn^{2+}/Cd^{2+} differentiation or discrimination see: (a) P. Li, X. Zhou, R. Huang, L. Yang, X. Tang, W. Dou, Q. Zhao and W. Liu, *Dalton Trans.*, 2014, **43**, 706; (b) Y. Tan, J. Gao, J. Yu, Z. Wang, Y. Cui, Y. Yang and G. Qian, *Dalton Trans.,* 2013, **42**, 11465; (c) M. C. Aragoni, M. Arca, A. Bencini, C. Caltagirone, A. Garau, F. Isaia, M. E. Light, V. Lippolis, C. Lodeiro, M. Mameli, R. Montis, M. C. Mostallino, A. Pintus and S. Puccioni, *Dalton Trans.*, 2013, **42**, 14516; (d) X. Liu, N. Zhang, J. Zhou, T. Chang, C. Fang and D. Shangguan, *Analyst*, 2013, **138**, 901.

14 U. Carpentieri, J. Myers, L. Thorpe, C. W. Daeschner III and M. E. Haggard, *Cancer Res.*, 1986, **46**, 981.

15 For papers dealing with Zn(II) selectivity over Cu(II): (a) Z. Dai, X. Xu and J. W. Canary, *Chem. Commun.*, 2002, **13**, 1414; (b) Z. Dai and J. W. Canary, *New J. Chem.*, 2007, **31**, 1708; (c) Y. Ding, Y. Xie, X. Li, J. P. Hill, W. Zhang and W. Zhu, *Chem. Commun.*, 2011, **47**, 5431; (d) D. A. Safin, M. G. Babashkina and Y. Garcia, *Dalton Trans.*, 2013, **42**, 1969; (e) K. E. Siters, M. A. Fountain and J. R. Morrow, *Inorg. Chem.*, 2014, **53**, 11540.

16 (a) S. Wang, B. Wu, F. Liu, Y. Gao and W. Zhang, *Polymer. Chem.*, 2015, **6**, 1127; (b) Z. Yang, M. She, J. Zhang, X. Chen, Y. Huang, H. Zhu, P. Liu, J. Li and Z. Shi, *Sensors Actuat. B*, 2013, **176**, 482; (c) H. Xiao, K. Chen, N. Jiang, D. Cui, G. Yin, J. Wang and R. Wang, *Analyst*, 2014, **139**, 1980. For reviews: (d) P. A. Vigato and S. Tamburini, *Coord. Chem. Rev.*, 2004, **248**, 1717; (e) N. Raman, S. Johnson and A. Sakthivel, *J. Coord. Chem.*, 2008, **62**, 691.

17 (a) Y. Fu, Q. C. Feng, X. J. Jiang, H. Xu, M. Li and S. Q. Zang, *Dalton Trans.*, 2014, **43**, 5815; (b) P. Saluja, N. Kaur, N. Singh and D. O. Jang, *Tetrahedron Lett.*, 2012, **53**, 3292; (c) X. W. Cao, W. Y. Lin and L. W. He, *Org. Lett.*, 2011, **13**, 4716; (d) L. Tanga and M. Cai, *Sens. Actuators, B*, 2012, **173**, 862.

18 O. Domínguez, B. Rodríguez-Molina, M. Rodríguez, A. Ariza, N. Farfán and R. Santillan, *New J. Chem.*, 2011, **35**, 156.

19 S. Fery-Forgues and D. Lavabre, *J. Chem. Educ.*, 1999, **76**, 1260.

20 (a) ATSDR, *"Toxicological profile"*, Agency for Toxic Substances and Disease Registry, **1999**, US Department of Health and Human Services. Public Health Service. Atlanta, Georgia, USA; (b) L. Friberg, C.G. Elinger and T. Kjellström *"Cadmium"*, World Health Organization, Genève, **1992**.

21 (a) P. Gans, A. Sabatini and A. Vacca, *Talanta*, 1996, **43**, 1739; (b) L. Alderighi, P. Gans, A. Ienco, D. Peters, A. Sabatini and A. Vacca, *Coord. Chem. Rev.*, 1999, **184**, 311.

22 (a) X. Qu, C. Li, H. Chen, J. Mack, Z. Guo and Z. Shen, *Chem. Commun.*, 2013, **49**, 7510; (b) M. Li, Q. Liang, M. Zheng, C. Fang, S. Peng and M. Zhao, *Dalton Trans.*, 2013, **42**, 13509.

23 R. K. Pathak, K. Tabbasum, A. Rai, D. Panda and C. P. Rao, *Anal. Chem.* 2012, **84**, 5117.

24 (a) S. K. Sahoo, D. Sharma, R. K. Bera, G. Crisponi and J. F. Callan, *Chem. Soc. Rev.*, 2012, **41**, 7195; (b) Y. Ma, V. Abbate, R. C. Hider, *Metallomics*, 2015, **7**, 212.

25 T. G. Ebrey, *Method. Enzymol.*, 2000, **315**, 196.

26 (a) K. Endre, N. Peter, A. B. S. Janos and M. Janos, *Cytometry*, 2008, **73A**, 559; (b) E. Tamanini, A. Katewa, L. M. Sedger, M. H. Todd and M. Watkinson, *Inorg. Chem.,* 2009, **48**, 319; (c) S. Johnson, V. Nguyen and D. Coder, *Curr. Protocol. Cytom.*, 2013, 9.2.1-9.2.26. DOI: 10.1002/0471142956.cy0902s64

27 (a) C. Amovilli, V. Barone, R. Cammi, E. Cancès, M. Cossi, B. Mennucci, C. S. Pomelli and J. Tomasi, *Adv. Quant. Chem.*, 1998, **32**, 227; (b) J. Tomasi, B. Mennucci and R. Cammi, *Chem. Rev.*, 2005, **105**, 2999.

28 M. J. Frisch, G. W. Trucks, H. B. Schlegel, G. E. Scuseria, M. A. Robb, J. R. Cheeseman, *et al.* Gaussian 03, Revision C.02, Wallingford CT, Gaussian, Inc., 2004.

29 C. Adamo and D. Jacquemin, *Chem. Soc. Rev.,* 2013, **42**, 845.

30 T. Le Bahers, C. Adamo and I. Ciofini, *J. Chem. Theory Comput.,* 2011, **7**, 2498.

31 R. L. Martin, *J. Chem. Phys.*, 2003, **118**, 4775.

32 (a) L. Fabbrizzi, M. Lichelli, P. Pallavicini, D. Sacchi and A. Taglietti, *Analyst*, 1996, **121**, 1763; and (b) *Chem. Eur. J.*, 1996, **2**, 75; (c) R. Bergonzi, L. Fabbrizzi, M. Lichelli and C. Mangano, *Coord. Chem. Rev.*, 1998, **170**, 31.

